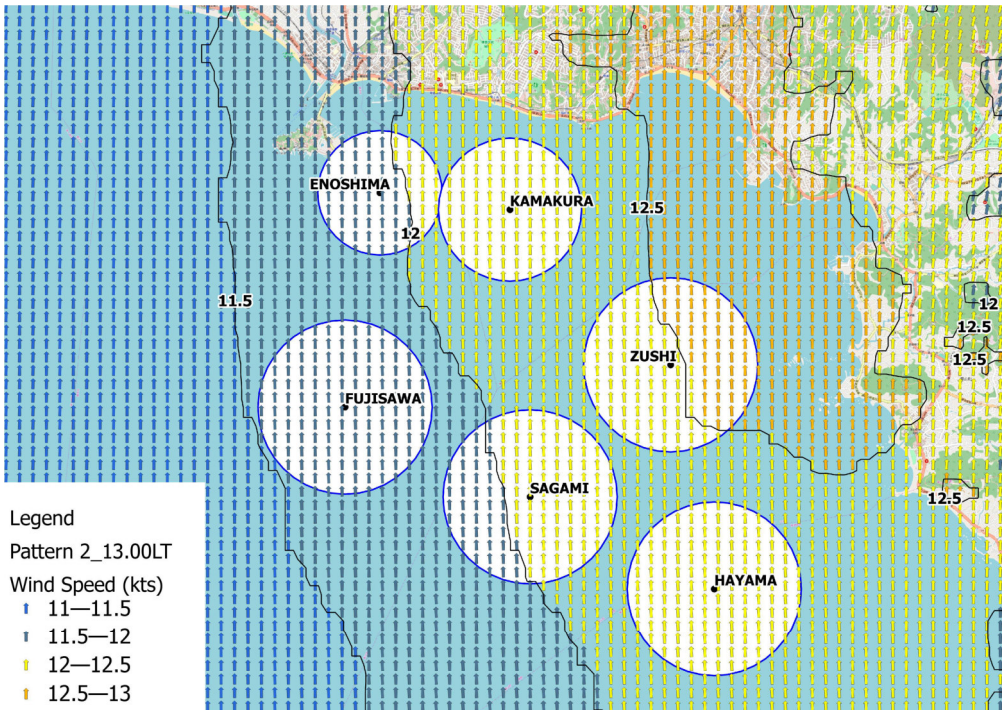

Figure 11. Modeled wind maps of the race fields: WP2—27.07.2016; 13.00 LT. The arrows represent the wind direction, the colors the speed. The isolines separate areas with different wind speed.

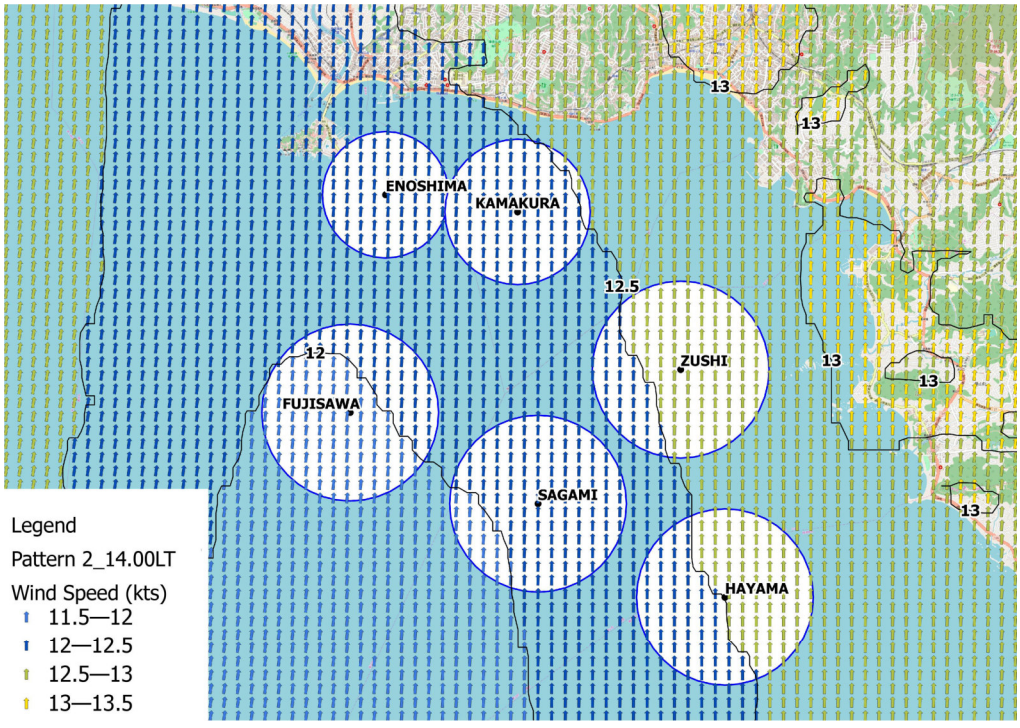

Figure 12. Modeled wind maps of the race fields: WP2—27.07.2016; 14.00 LT. The arrows represent the wind direction, the colors the speed. The isolines separate areas with different wind speed.

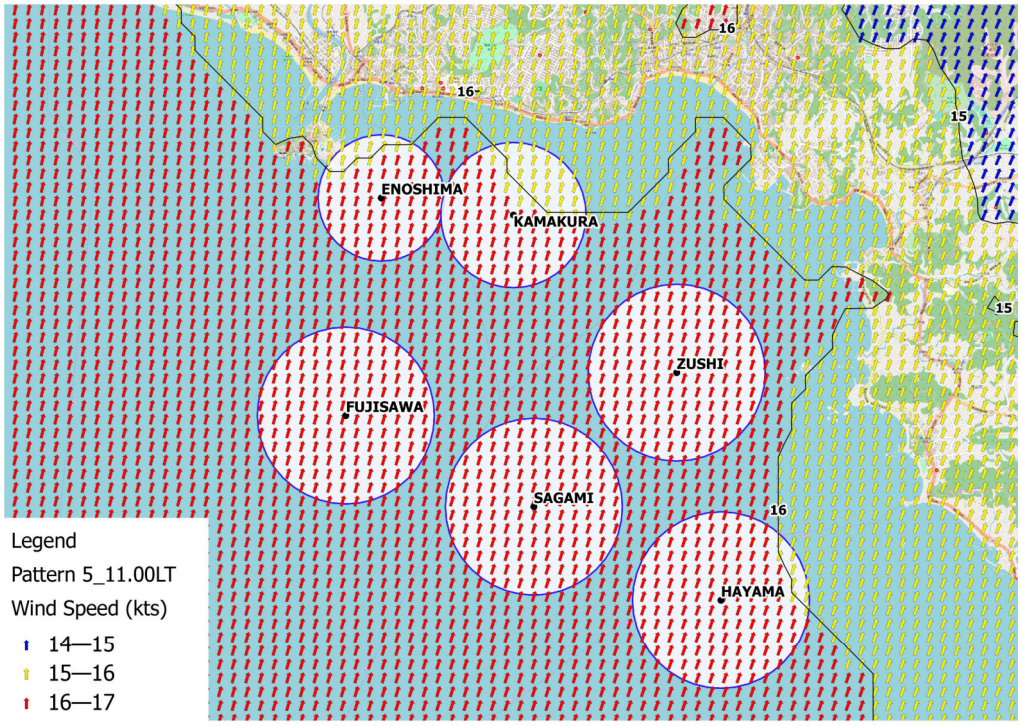

Figure 13. Modeled wind maps of the race fields: WP5—28.07.2010; 11.00 LT. The arrows represent the wind direction, the colors the speed. The isolines separate areas with different wind speed.

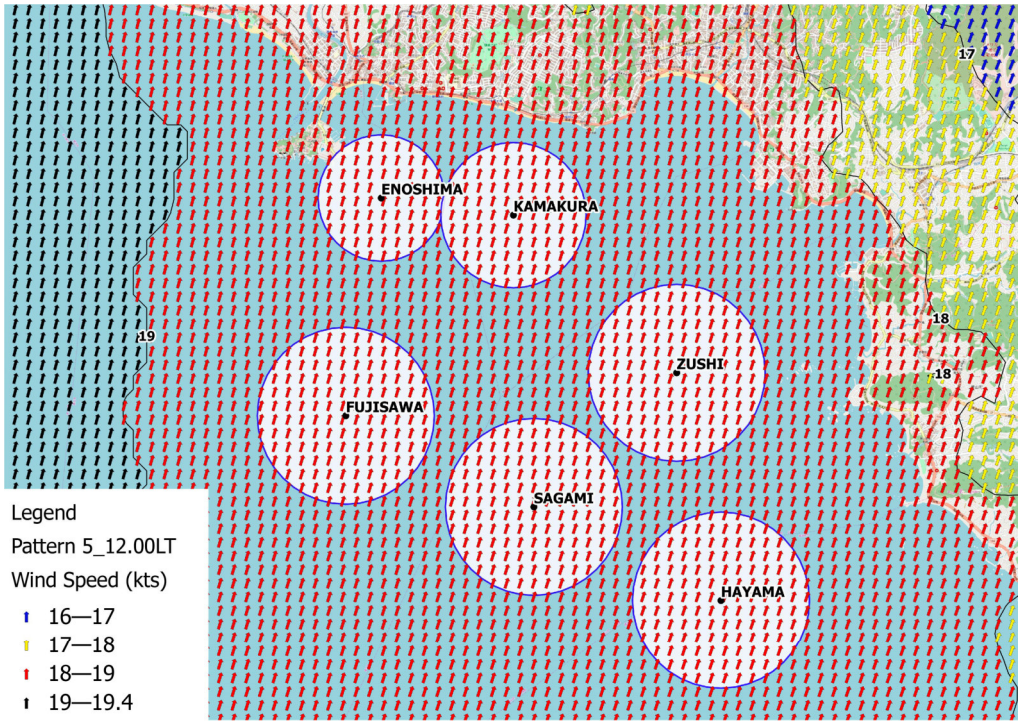

Figure 14. Modeled wind maps of the race fields: WP5—28.07.2010; 12.00 LT. The arrows represent the wind direction, the colors the speed. The isolines separate areas with different wind speed.

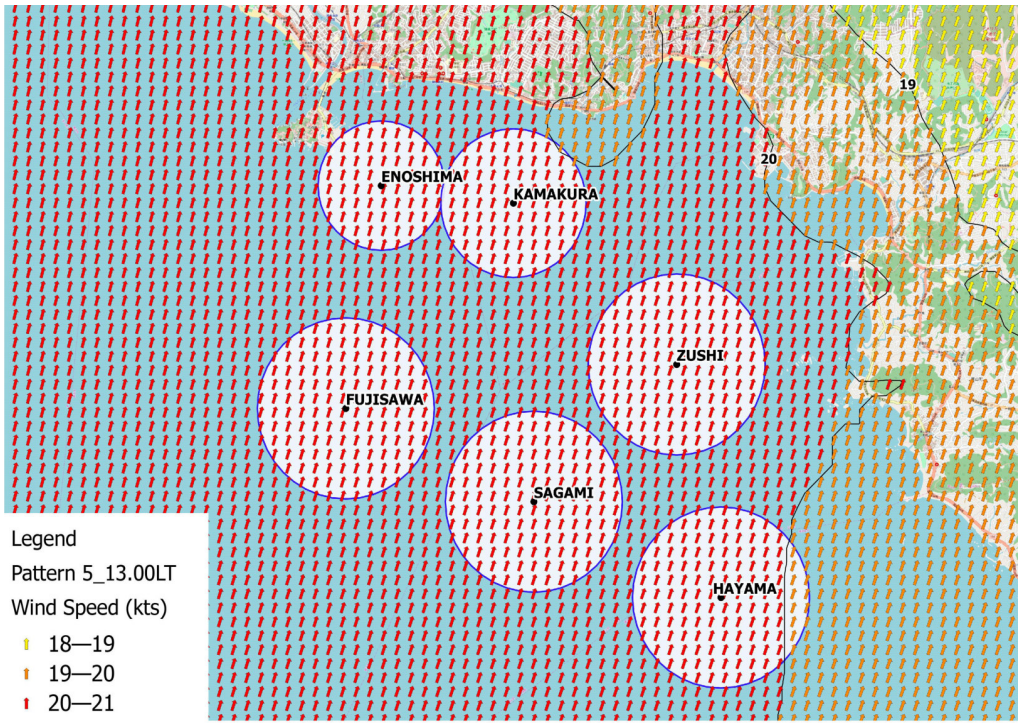

Figure 15. Modeled wind maps of the race fields: WP5—28.07.2010; 13.00 LT. The arrows represent the wind direction, the colors the speed. The isolines separate areas with different wind speed.

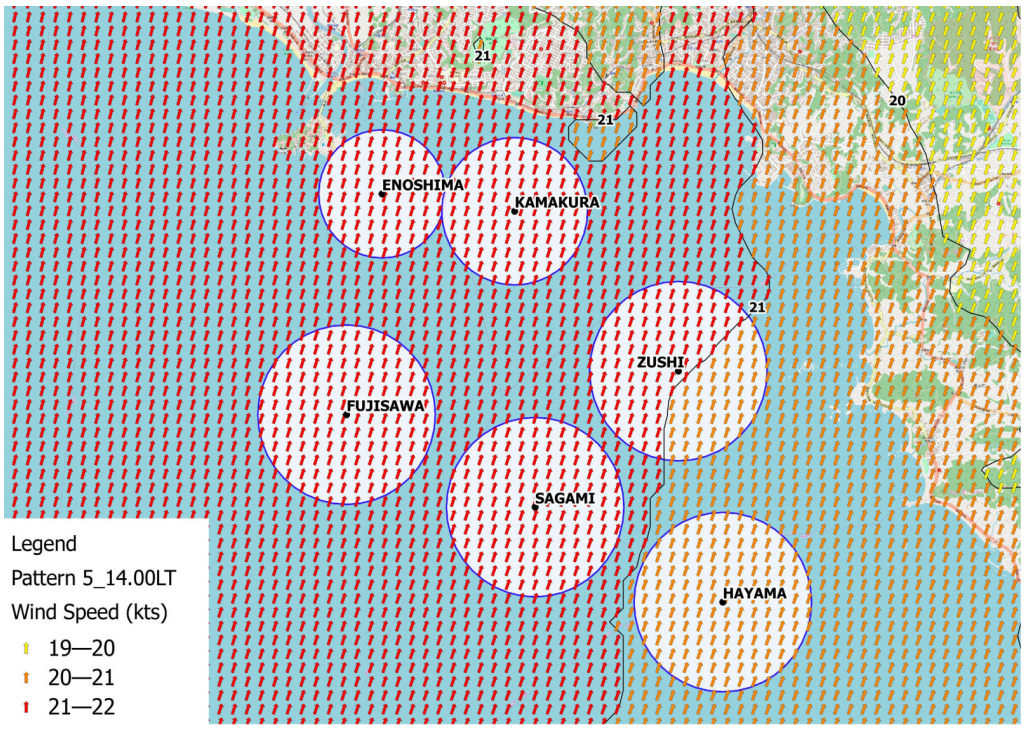

Figure 16. Modeled wind maps of the race fields: WP5—28.07.2010; 14.00 LT. The arrows represent the wind direction, the colors the speed. The isolines separate areas with different wind speed.

Finally, we summarized all the analyzed data into a final table that gives the necessary indications to the athletes on how best to approach the different wind conditions. Tables 6–8 show the tables of WP1A, WP2, and WP5, respectively.

Table 6. WP1A. Warnings for sailors.

Gradient wind (1000 m)	NE/6–9 kts
Wind direction (max. left)	180–190 (starting sea breeze around 11.00 ÷ 12.00LT) 160–170 (at the end of the day)
Wind direction (max. right)	225–235
Wind speed (min.) [kts]	5–6 (starting sea breeze around 11.00 ÷ 12.00LT)
Wind speed (max.) [kts]	10–12 (at the end of the day)
Shift	After the FIRST SHIFT (BACKING if the wind direction will be more right than 180–190 or VEERING if the wind direction will be more left than 180–190), expected around 12.00LT, the wind will VEERING to reach the maximum right (expected around 15.00LT), then it will be BACKING. ATTENTION 1: During the VEERING and the BACKING, the wind will be OSCILLATING (in the start period of the sea breeze around 12.00LT: period around 5′–10′ with angle between 002°–005°; after 14.00–15.00LT: the oscillations will be bigger in period, 10′–15′, and in angle around 005°–008°, max. 010°). ATTENTION 2: The wind speed will increase all days both in VEERING and BACKING
Wind pressure	When the sea breeze starting and for all day (both in VEERING and BACKING), the good pressure will be on the right hand side.
Wave—Swell	SSW wind-wave with possible SW swell
Air temperature (Ta) & Sea Temperature (Ts)	Ta = 26 ÷ 30° C (increasing) Ts = 25 ÷ 26° C (min. 23° C; max. 28° C)
Atmospheric pressure	Increasing in the morning, then steady and finally decreasing from the early afternoon.
Sky and clouds	Clear with good visibility in the morning, then cumulus (Cu) steady inland.
Occurrence's frequencies	40.6% (together with WP1_B and WP1_C)

Table 7. WP2. Warnings for sailors.

Gradient wind (1000 m)	S-SW/1–9kts
Wind direction (max. left)	160–170 (with the minimum of the wind speed included between 5–7 kts) 170–180 (with the minimum of the wind speed included between 5–7 kts)
Wind direction (max. right)	220–230
Wind speed (min.) [kts]	5–6 A significant measure of the minimum of the wind speed will be around 12.00LT
Wind speed (max.) [kts]	11–13
Shift	LEFT trend until 12.00 ÷ 13.00LT, then RIGHT trend in OSCILLATING wind (long oscillations, more or less 10′–20′ as the persistent shifts, with big angle included between 020°–040°. It will be very difficult to find an average direction due to the long period of the oscillations). ATTENTION FOR THE OSCILLATIONS: Danger! It is very difficult to know the period of the oscillations, so it is very difficult to be well positioned in function of the oscillations. We do not have "secondary" OSCILLATIONS to help us to *return* if we are on the wrong side. You have to be careful!
Wind pressure	Zushi better pressure in left hand side; Sagami possible better on left hand side (it depends on the strength of the wind speed); in other race areas, better in the middle right but, sometimes the pressure follows the shift.
Wave—Swell	SW
Air temperature (Ta) & Sea Temperature (Ts)	Ta = 26 ÷ 30° C (increasing) Ts = 25 ÷ 26° C (min. 23° C; max. 28° C)
Atmospheric pressure	Decreasing
Sky and clouds	Partially cloudy with milky sky and bad visibility. Stratocumulus (Sc) and Cu clouds in race area.
Occurrence's frequencies	31.8%

Table 8. WP5. Warnings for sailors.

Gradient wind (1000 m)	SW/10–15 kts (moderate) SW/16–25 kts (strong)
Wind direction (max. left)	180–190
Wind direction (max. right)	220–230 (early morning or in the start of the pattern) 200–210 (late afternoon or in the end of the pattern)
Wind speed (min.) [kts]	10–11
Wind speed (max.) [kts]	20–25 G 30
Shift	First trend to the LEFT (with increasing wind speed). Then, when the wind speed is above 14–15kts, OSCILLATING wind (oscillations, more or less 5′–20′ as the persistent shifts, with the angle included between 010°–020°. It will be very difficult to find an average direction due to the long period of the oscillations) with slight RIGHT trend in the end of the day. ATTENTION FOR THE OSCILLATIONS: Danger! It is very difficult to know the period of the oscillations, so it is very difficult to be well positioned in function of the oscillations. We do not have "secondary" OSCILLATIONS to help us to *return* if we are on the wrong side. You have to be careful! ATTENTION FOR THE STRATEGY 1: If you start at 12.00LT, a good side will be the middle left for the first shift and the good pressure from left. If you start later (from 13.00 to 16.00LT), the situation will be OPEN. The best solution is sailing fast in the center of the race area (middle right can be favored but also middle left is safe). AVOID THE CORNER! ATTENTION FOR THE STRATEGY 1: In the Fujisawa race area, the increasing wind speed (from 11–12 kts to 16–17 kts) or in decreasing wind speed (from 18–19 kts to 11–12 kts), the best side is the left for the pressure and for the left hand shift of the wind in the top-mark (left wind in the top-mark comparing to the start line). In this case, YOU CAN SAIL HARD IN THE CORNER!
Wind pressure	In the first moment, when the wind speed increases up to 13–15 kts and shift left, the good pressure is in the left hand side, then the good pressure gradually moves to the off-shore race area and in the right hand side for Zushi and Hayama. In other race areas (excluding Fujisawa), the pressure is almost the same forboth for right and left hand side. In Fujisawa, it is better on the left hand side.
Wave—Swell	SW wind-wave and swell
Air temperature (Ta) & Sea Temperature (Ts)	Ta = 26 ÷ 32° C (increasing) Ts = 25 ÷ 26° C (min. 23° C; max. 28° C)
Atmospheric pressure	Decreasing
Sky and clouds	Partially cloudy–cloudy with front moving on the race area or clear partially cloudy with medium visibility and Cu, Cumulonimbus (Cb), steady inland and along the coastal line in the afternoon
Occurrence's frequencies	10.2%

These tables were generated using the information derived from the results of the CALMET model and starting from the gradient wind extracted by the NOAA-GFS gradient wind. It is evident, looking at Figures 5–16, how we can summarize in "meta-communication" called "wind's pressure" the distribution of the wind speed in the different race area. At the same time, the analysis of the CALMET results in the different time slot helps to generate an abstract of the wind's shifts that are crucial for the strategical decision.

Finally, considering all the possible information that can be extracted from the wind patterns tables (i.e., trend of the atmospheric pressure and difference between air temperature and sea temperature), it is possible to have a more detailed analysis of the oscillations patterns that cannot be shown by the results of the CALMET model.

Once all the data were updated and organized in plots, tables, and maps, we could finally build the new version of the "call book". These kinds of instruments are essential in the preparation of competitions since they represent the connection between scientific research and sports performance.

4. Discussion

The methodology developed in this research provides an in-depth knowledge of the meteorological variables, and in sports where these variables have a strong influence such as sailing, it can help athletes to prepare a race strategy. This method is divided into three

main steps, and the outcome can give a significant advantage during competitions to the athletes who apply it.

First, a simulation was run through a NWP system to reconstruct a database of weather conditions in the selected area. For this study, we chose the WRF and CALMET models, whose combined use has proven to be one of the most effective tools in forecasting meteorological variables. One advantage of these models is that they can run almost in real time, between 12 and 24 h before the event. Thereafter, the WP of the day will be determined by comparing the gradient wind, predicted and observed, by the JMA wind profiler.

The second step concerns the analysis of the data extracted from the database. Initially, we used the simulated data to reconstruct the most frequent wind patterns inside the bay; then we tested the model, comparing the simulated data with those collected in the field. The results of the statistical analysis—performed by means of BIAS, MAE, and PCC—also allowed us to identify the simulated days with the highest level of accuracy, which were used for the creation of wind maps on QGIS.

Finally, the data are presented and communicated. The tool through which this last phase is carried out is the "call book", a guide that provides, for each pattern, data and information concerning all the relevant meteorological variables, in a clear and synthetic way. This tool is used by the coaches during training as a decision support service to prepare the regatta strategy, but it can also be very useful on the race day, when compared to the short-term weather forecast, to know in advance the developments of the weather conditions.

During the Olympic Test Event held in Enoshima in August 2019, the "call book" was used to prepare the forecasts and to decide the race strategies for the Swedish Sailing Olympic Team. The results obtained by the Team (one gold medal in Laser class and one silver medal in 470 class), together with a re-analysis conducted with the data measured by the SAP system (https://www.sapsailing.com/gwt/Home.html#/event/:eventId=6389fb9d-12e1-47ef-9831-ddab8cf9598f, last access: 11 May 2021), showed for us that the "call book" had a higher reliability estimated around 80%. This analysis indicated that the applied methodology can be considered robust, considering the limitation that the results of the model have to be summarized in a single table. In the case of complex topography and considering that the races are in different areas, an abstract of the information in a single table can generate a loss of information. Of course, to minimize this risk, a continuous feedback between athletes, coaches and meteorologist is very important as we applied it to build the presented "call book".

Finally, the results show how a methodology, utilized in other research areas, can be considered innovative in the sport field. At the same time, it is interesting to observe that climatic analysis can be extended to an unusual application, which is the sport industry. Moreover, it is important to observe that this methodology can be applied to study the climatic conditions of the coastal area regarding the management of offshore works.

5. Conclusions

In this research, the recurring weather conditions inside Enoshima Bay in Japan were analyzed. The time-period examined was the one in which the 2020 Tokyo Olympics were supposed to take place from 24 July to 9 August. This analysis is part of a wider system that, through scientific research, aims to improve the sports performance of athletes. This paper focused on sailing competitions, but the same methodology can be applied to other sports.

Through the CALWRF processor, a combined simulation of the WRF and CALMET models was launched, thanks to which we built an offshore database of the recent 10-year period, from 2009 to 2018. From this dataset, we extracted, in the time interval that goes from 9.00LT to 18.00 LT, data of wind direction and wind speed at 10 m above sea level. Furthermore, we extracted the air temperature and density near the ground to estimate the atmospheric pressure employed to build the ternary plots and identify the wind patterns.

The CALMET output was processed with WindRose PRO3 software to classify the different wind behavior scenarios according to wind speed and direction. At the beginning, we created wind roses for all race fields, which showed a similar behavior: prevailing wind direction from S and SSW and a constant increase in speed during the day. Afterward, we constructed the ternary plots, comparing wind speed and direction and atmospheric pressure; this allowed us to identify six distinct patterns.

Once the wind patterns were established, we conducted a climatological analysis using NOAA data to select the days that best fit the pattern perimeters. From this analysis, we selected and extracted from the CALMET database 32 days, on which the model verification was carried out. The comparison between the data extracted from CALMET and those observed during the summer of 2019 was performed, applying three statistical indexes: BIAS, MAE, and PCC.

The results of the statistical analysis demonstrated the high reliability of the model in predicting wind behavior. On the day selected to represent the WP2, the average error of wind direction was around 14 degrees, while the average error of wind speed was below 4 kts; the average PCC value was about 0.4 for the wind direction 0.6 for the speed. We reiterated this type of analysis for each pattern, always selecting the day that produced the best results. With the data of the selected days, we created the wind maps, graphs, and tables to fill the "call book", the final guide with highly detailed information needed by sailors.

This method brings two elements of great innovation to this research area: the use of historical data, simulated with CALMET, as climate data and its capacity for continuous improvement by correcting past mistakes.

This is a completely new system and future research needs to improve it. For example, the quality of the weather database might be improved by adding the measurements of weather stations, with nudging techniques in WRF, or directly in CALMET as surface stations; moreover, the verification of hind-cast could be integrated with other statistical models.

In addition, this analysis might be applied to other research fields. For instance, we believe that the knowledge of the wind patterns could be valuable in studying climate change effects in marine and coastal area to design the best adaption and mitigation initiatives.

Author Contributions: Conceptualization, A.P., R.B.(Roberto Bellasio) and P.M.; Methodology, P.M., A.P., R.B. (Roberto Bellasio), R.B. (Roberto Bianconi) and A.B.; Modeling, R.B. (Roberto Bellasio) and R.B. (Roberto Bianconi); Validation, P.M., A.P., R.B. (Roberto Bellasio) and A.B.; Formal analysis, A.P. and P.M.; Graphical analysis (QGIS), P.M., A.P. and A.B.; Writing—original draft preparation, P.M., A.P. and R.B. (Roberto Bellasio); Writing—review and editing, A.P., R.B. (Roberto Bellasio) and A.B.; Supervision, A.P.; Project management, A.P. All authors have read and agreed to the published version of the manuscript.

Funding: This research received no external funding.

Acknowledgments: The authors acknowledge the Swedish Sailing Federation for the support to the presented research.

Conflicts of Interest: The authors declare no conflict of interest.

Appendix A

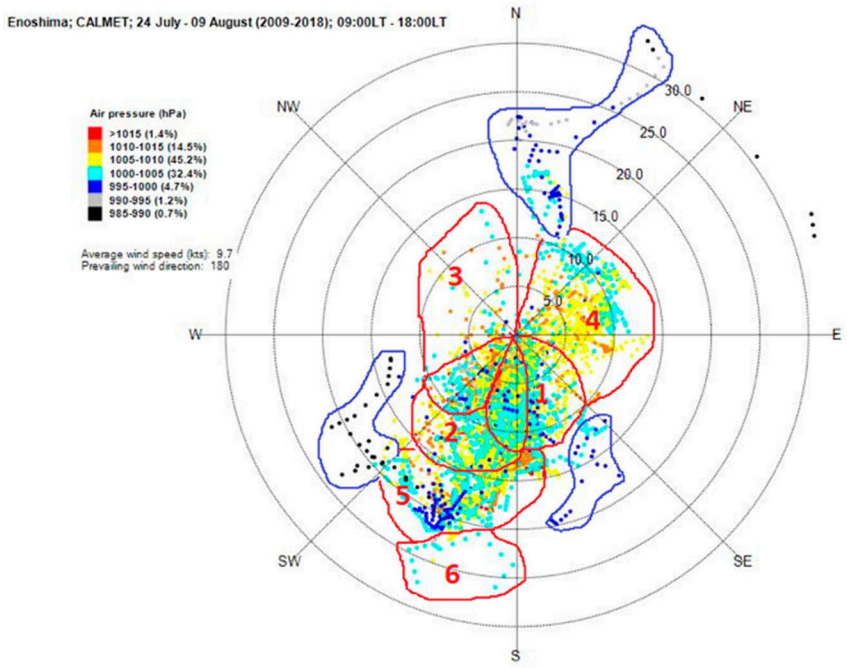

Figure A1. Ternary plot with wind direction (deg), wind speed (kts), and air pressure (hPa) for the Enoshima race area generated by CALMET. Time interval 09:00LT–18:00LT, period 24 July–9 August, years 2009–2018.

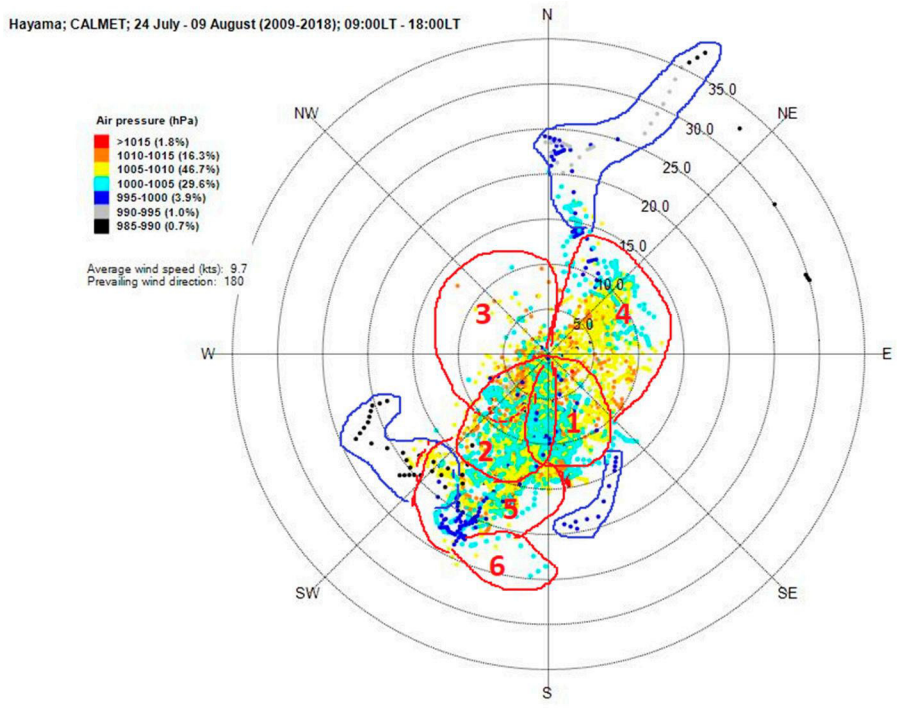

Figure A2. Ternary plot with wind direction (deg), wind speed (kts), and air pressure (hPa) for the Hayama race area generated by CALMET. Time interval 09:00LT–18:00LT, period 24 July–9 August, years 2009–2018.

Appendix B

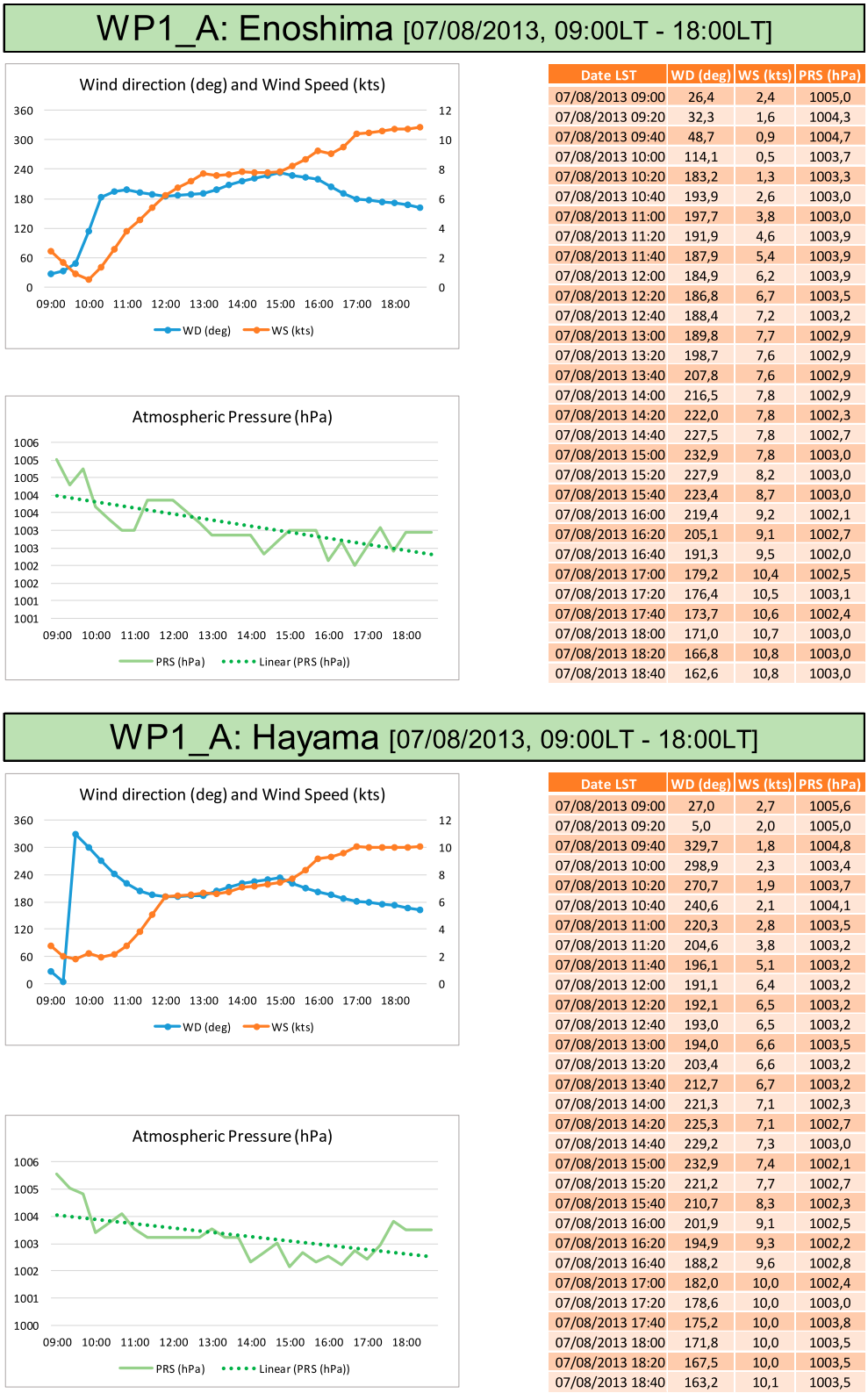

Date LST	WD (deg)	WS (kts)	PRS (hPa)
07/08/2013 09:00	26,4	2,4	1005,0
07/08/2013 09:20	32,3	1,6	1004,3
07/08/2013 09:40	48,7	0,9	1004,7
07/08/2013 10:00	114,1	0,5	1003,7
07/08/2013 10:20	183,2	1,3	1003,3
07/08/2013 10:40	193,9	2,6	1003,0
07/08/2013 11:00	197,7	3,8	1003,0
07/08/2013 11:20	191,9	4,6	1003,9
07/08/2013 11:40	187,9	5,4	1003,9
07/08/2013 12:00	184,9	6,2	1003,9
07/08/2013 12:20	186,8	6,7	1003,5
07/08/2013 12:40	188,4	7,2	1003,2
07/08/2013 13:00	189,8	7,7	1002,9
07/08/2013 13:20	198,7	7,6	1002,9
07/08/2013 13:40	207,8	7,6	1002,9
07/08/2013 14:00	216,5	7,8	1002,9
07/08/2013 14:20	222,0	7,8	1002,3
07/08/2013 14:40	227,5	7,8	1002,7
07/08/2013 15:00	232,9	7,8	1003,0
07/08/2013 15:20	227,9	8,2	1003,0
07/08/2013 15:40	223,4	8,7	1003,0
07/08/2013 16:00	219,4	9,2	1002,1
07/08/2013 16:20	205,1	9,1	1002,7
07/08/2013 16:40	191,3	9,5	1002,0
07/08/2013 17:00	179,2	10,4	1002,5
07/08/2013 17:20	176,4	10,5	1003,1
07/08/2013 17:40	173,7	10,6	1002,4
07/08/2013 18:00	171,0	10,7	1003,0
07/08/2013 18:20	166,8	10,8	1003,0
07/08/2013 18:40	162,6	10,8	1003,0

Date LST	WD (deg)	WS (kts)	PRS (hPa)
07/08/2013 09:00	27,0	2,7	1005,6
07/08/2013 09:20	5,0	2,0	1005,0
07/08/2013 09:40	329,7	1,8	1004,8
07/08/2013 10:00	298,9	2,3	1003,4
07/08/2013 10:20	270,7	1,9	1003,7
07/08/2013 10:40	240,6	2,1	1004,1
07/08/2013 11:00	220,3	2,8	1003,5
07/08/2013 11:20	204,6	3,8	1003,2
07/08/2013 11:40	196,1	5,1	1003,2
07/08/2013 12:00	191,1	6,4	1003,2
07/08/2013 12:20	192,1	6,5	1003,2
07/08/2013 12:40	193,0	6,5	1003,2
07/08/2013 13:00	194,0	6,6	1003,5
07/08/2013 13:20	203,4	6,6	1003,2
07/08/2013 13:40	212,7	6,7	1003,2
07/08/2013 14:00	221,3	7,1	1002,3
07/08/2013 14:20	225,3	7,1	1002,7
07/08/2013 14:40	229,2	7,3	1003,0
07/08/2013 15:00	232,9	7,4	1002,1
07/08/2013 15:20	221,2	7,7	1002,7
07/08/2013 15:40	210,7	8,3	1002,3
07/08/2013 16:00	201,9	9,1	1002,5
07/08/2013 16:20	194,9	9,3	1002,2
07/08/2013 16:40	188,2	9,6	1002,8
07/08/2013 17:00	182,0	10,0	1002,4
07/08/2013 17:20	178,6	10,0	1003,0
07/08/2013 17:40	175,2	10,0	1003,8
07/08/2013 18:00	171,8	10,0	1003,5
07/08/2013 18:20	167,5	10,0	1003,5
07/08/2013 18:40	163,2	10,1	1003,5

Figure A3. WP1A, Enoshima and Hayama race field, 07/08/2013. Wind speed and direction and atmospheric pressure data extracted and simulated on CALMET.

WP2: Enoshima [27/07/2016, 09:00LT - 18:00LT]

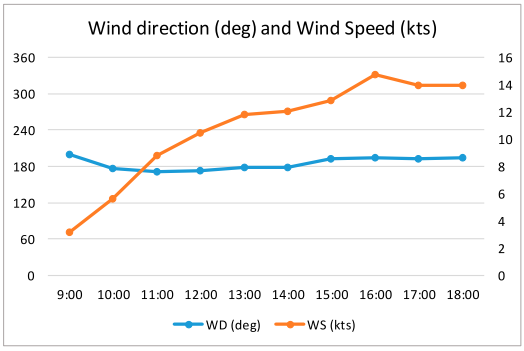

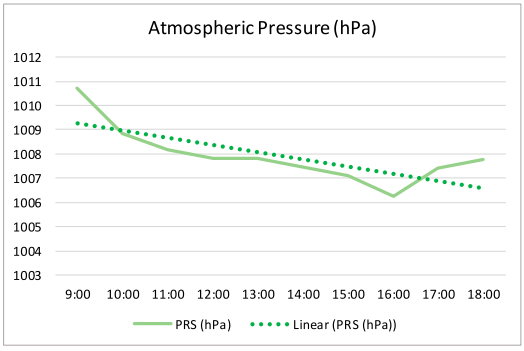

Date LST	WD (deg)	WS (kts)	PRS (hPa)
27/07/2016 09:00	200,1	3,1	1010,7
27/07/2016 09:20	188,7	3,9	1010,2
27/07/2016 09:40	181,1	4,7	1009,4
27/07/2016 10:00	175,9	5,6	1008,9
27/07/2016 10:20	173,8	6,7	1008,3
27/07/2016 10:40	172,2	7,7	1008,7
27/07/2016 11:00	171,1	8,8	1008,2
27/07/2016 11:20	172,1	9,3	1007,7
27/07/2016 11:40	173	9,9	1008,3
27/07/2016 12:00	173,8	10,4	1007,8
27/07/2016 12:20	175,4	10,9	1007,7
27/07/2016 12:40	177	11,3	1008,0
27/07/2016 13:00	178,4	11,8	1007,8
27/07/2016 13:20	178,6	11,9	1007,3
27/07/2016 13:40	178,8	11,9	1007,6
27/07/2016 14:00	179,1	12,0	1007,5
27/07/2016 14:20	183,6	12,2	1006,9
27/07/2016 14:40	187,9	12,5	1007,6
27/07/2016 15:00	192	12,8	1007,1
27/07/2016 15:20	193,1	13,5	1007,1
27/07/2016 15:40	194	14,1	1007,1
27/07/2016 16:00	194,8	14,7	1006,2
27/07/2016 16:20	194,2	14,4	1006,6
27/07/2016 16:40	193,5	14,2	1007,4
27/07/2016 17:00	192,7	13,9	1007,4
27/07/2016 17:20	193	13,9	1007,8
27/07/2016 17:40	193,2	13,9	1007,8
27/07/2016 18:00	193,5	13,9	1007,8
27/07/2016 18:20	194,6	13,6	1007,8
27/07/2016 18:40	195,8	13,4	1007,8

WP2: Hayama [27/07/2016, 09:00LT - 18:00LT]

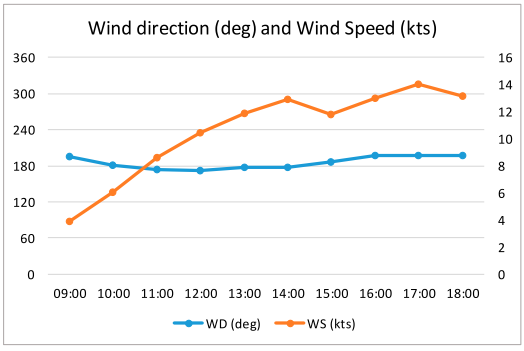

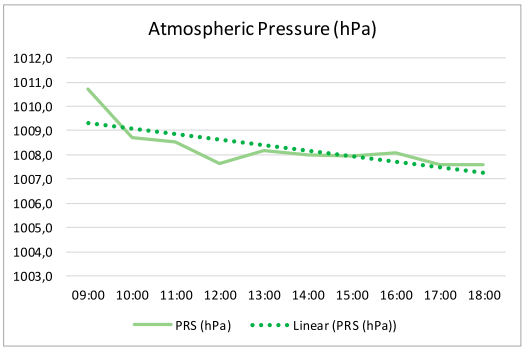

Date LST	WD (deg)	WS (kts)	PRS (hPa)
27/07/2016 09:00	195,2	3,9	1010,7
27/07/2016 09:20	189,1	4,6	1010,2
27/07/2016 09:40	184,6	5,3	1009,7
27/07/2016 10:00	181,3	6,0	1008,7
27/07/2016 10:20	177,8	6,9	1008,7
27/07/2016 10:40	175,2	7,7	1009,0
27/07/2016 11:00	173,1	8,6	1008,5
27/07/2016 11:20	172,7	9,2	1008,3
27/07/2016 11:40	172,4	9,8	1007,8
27/07/2016 12:00	172,1	10,5	1007,7
27/07/2016 12:20	174,2	10,9	1008,0
27/07/2016 12:40	176,2	11,4	1007,8
27/07/2016 13:00	178	11,9	1008,2
27/07/2016 13:20	177,6	12,2	1007,6
27/07/2016 13:40	177,3	12,5	1007,6
27/07/2016 14:00	177	12,9	1008,0
27/07/2016 14:20	180	12,5	1007,8
27/07/2016 14:40	183,1	12,1	1007,3
27/07/2016 15:00	186,4	11,8	1007,9
27/07/2016 15:20	190,3	12,1	1007,4
27/07/2016 15:40	194	12,5	1007,8
27/07/2016 16:00	197,4	13,0	1008,1
27/07/2016 16:20	197,3	13,3	1008,1
27/07/2016 16:40	197,1	13,7	1007,6
27/07/2016 17:00	197	14,0	1007,6
27/07/2016 17:20	197	13,7	1007,6
27/07/2016 17:40	197	13,4	1007,6
27/07/2016 18:00	197	13,1	1007,6
27/07/2016 18:20	196,6	12,8	1008,4
27/07/2016 18:40	196,2	12,5	1008,4

Figure A4. WP2, Enoshima and Hayama race field, 27/07/2016. Wind speed and direction and atmospheric pressure data extracted and simulated on CALMET.

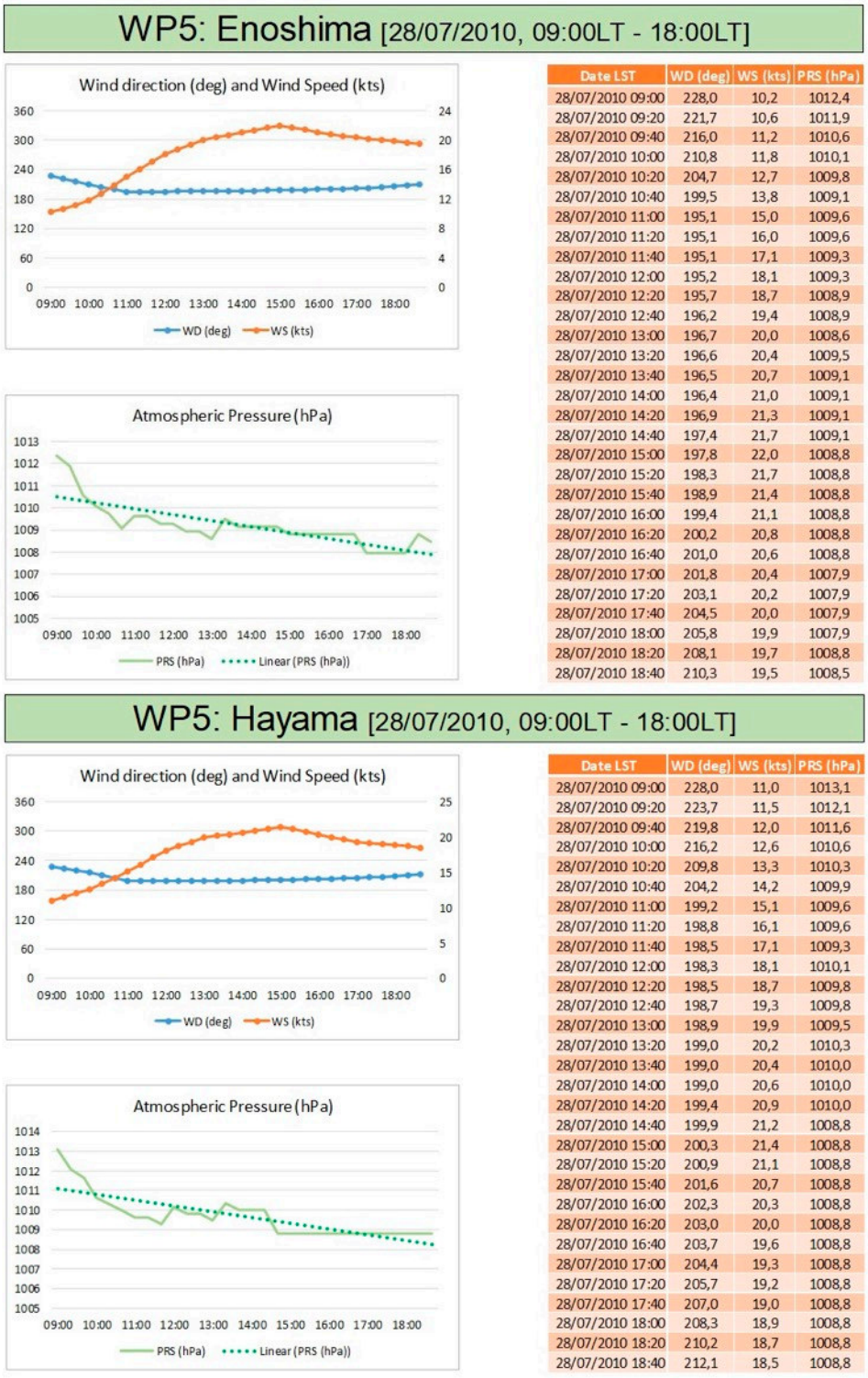

Date LST	WD (deg)	WS (kts)	PRS (hPa)
28/07/2010 09:00	228,0	10,2	1012,4
28/07/2010 09:20	221,7	10,6	1011,9
28/07/2010 09:40	216,0	11,2	1010,6
28/07/2010 10:00	210,8	11,8	1010,1
28/07/2010 10:20	204,7	12,7	1009,8
28/07/2010 10:40	199,5	13,8	1009,1
28/07/2010 11:00	195,1	15,0	1009,6
28/07/2010 11:20	195,1	16,0	1009,6
28/07/2010 11:40	195,1	17,1	1009,3
28/07/2010 12:00	195,2	18,1	1009,3
28/07/2010 12:20	195,7	18,7	1008,9
28/07/2010 12:40	196,2	19,4	1008,9
28/07/2010 13:00	196,7	20,0	1008,6
28/07/2010 13:20	196,6	20,4	1009,5
28/07/2010 13:40	196,5	20,7	1009,1
28/07/2010 14:00	196,4	21,0	1009,1
28/07/2010 14:20	196,9	21,3	1009,1
28/07/2010 14:40	197,4	21,7	1009,1
28/07/2010 15:00	197,8	22,0	1008,8
28/07/2010 15:20	198,3	21,7	1008,8
28/07/2010 15:40	198,9	21,4	1008,8
28/07/2010 16:00	199,4	21,1	1008,8
28/07/2010 16:20	200,2	20,8	1008,8
28/07/2010 16:40	201,0	20,6	1008,8
28/07/2010 17:00	201,8	20,4	1007,9
28/07/2010 17:20	203,1	20,2	1007,9
28/07/2010 17:40	204,5	20,0	1007,9
28/07/2010 18:00	205,8	19,9	1007,9
28/07/2010 18:20	208,1	19,7	1008,8
28/07/2010 18:40	210,3	19,5	1008,5

Date LST	WD (deg)	WS (kts)	PRS (hPa)
28/07/2010 09:00	228,0	11,0	1013,1
28/07/2010 09:20	223,7	11,5	1012,1
28/07/2010 09:40	219,8	12,0	1011,6
28/07/2010 10:00	216,2	12,6	1010,6
28/07/2010 10:20	209,8	13,3	1010,3
28/07/2010 10:40	204,2	14,2	1009,9
28/07/2010 11:00	199,2	15,1	1009,6
28/07/2010 11:20	198,8	16,1	1009,6
28/07/2010 11:40	198,5	17,1	1009,3
28/07/2010 12:00	198,3	18,1	1010,1
28/07/2010 12:20	198,5	18,7	1009,8
28/07/2010 12:40	198,7	19,3	1009,8
28/07/2010 13:00	198,9	19,9	1009,5
28/07/2010 13:20	199,0	20,2	1010,3
28/07/2010 13:40	199,0	20,4	1010,0
28/07/2010 14:00	199,0	20,6	1010,0
28/07/2010 14:20	199,4	20,9	1010,0
28/07/2010 14:40	199,9	21,2	1008,8
28/07/2010 15:00	200,3	21,4	1008,8
28/07/2010 15:20	200,9	21,1	1008,8
28/07/2010 15:40	201,6	20,7	1008,8
28/07/2010 16:00	202,3	20,3	1008,8
28/07/2010 16:20	203,0	20,0	1008,8
28/07/2010 16:40	203,7	19,6	1008,8
28/07/2010 17:00	204,4	19,3	1008,8
28/07/2010 17:20	205,7	19,2	1008,8
28/07/2010 17:40	207,0	19,0	1008,8
28/07/2010 18:00	208,3	18,9	1008,8
28/07/2010 18:20	210,2	18,7	1008,8
28/07/2010 18:40	212,1	18,5	1008,8

Figure A5. WP5, Enoshima and Hayama race field, 28/07/2010. Wind speed and direction and atmospheric pressure data extracted simulated on CALMET.

References

1. Hagen, L.J. Evaluation of the Wind Erosion Prediction System (WEPS) erosion submodel on cropland fields. *Environ. Model. & Softw.* **2004**, *19*, 171–176.
2. Weber, R.W. Meteorologic variables in aerobiology. *Immunol. Allergy Clin. N. Am.* **2003**, *23*, 411–422. [CrossRef]
3. Cogliani, E. Air pollution forecast in cities by an air pollution index highly correlated with meteorological variables. *Atmos. Environ.* **2001**, *35*, 2871–2877. [CrossRef]

4. Traveria, M.; Escribano, A.; Palomo, P. Statistical wind forecast for Reus airport. *Meteorol. Appl.* **2010**, *17*, 485–495. [CrossRef]
5. Bellasio, R. Analysis of wind data for airport runway design. *J. Airl. Airpt. Manag.* **2014**, *4*, 97–116. [CrossRef]
6. Olayinka, A.S.; Ukhurebor, K.E.; Ogunmola, K.; Aruewamedo, K. Effects of Meteorological Variables on the Efficiency of Solar Panel. *J. Niger. Assoc. Math. Phys.* **2018**, *4*.
7. Xu, W.; Ning, L.; Luo, Y. Wind Speed Forecast Based on Post-Processing of Numerical Weather Predictions Using a Gradient Boosting Decision Tree Algorithm. *Atmosphere* **2020**, *11*, 738. [CrossRef]
8. El Helou, N.; Tafflet, M.; Berthelot, G.; Tolaini, J.; Marc, A.; Guillaume, M.; Hausswirth, C.; Toussaint, J.F. Impact of environmental parameters on marathon running performance. *PLoS ONE* **2012**, *7*, e37407. [CrossRef]
9. Pezzoli, A.; Cristofori, E.; Gozzini, B.; Marchisio, M.; Padoan, J. Analysis of the thermal comfort in cycling athletes. *Procedia Eng.* **2012**, *34*, 433–438. [CrossRef]
10. Peiffer, J.J.; Abbiss, C.R. Influence of environmental temperature on 40 km cycling time-trial performance. *Int. J. Sports Physiol. Perform.* **2011**, *6*, 208–220. [CrossRef]
11. Buchheit, M.; Voss, S.C.; Nybo, L.; Mohr, M.; Racinais, S. Physiological and performance adaptations to an in-season soccer camp in the heat: Associations with heart rate and heart rate variability. *Scand. J. Med. Sci. Sports* **2011**, *21*, 477–485. [CrossRef] [PubMed]
12. Pezzoli, A.; Bellasio, R. Computer supported analysis of thermal comfort for cycling sport. *Sport Sci. Res. Technol. Support* **2016**, 71–85.
13. Golding, B.W.; Ballard, S.P.; Mylne, K.; Roberts, N.; Saulter, A.; Wilson, C.; Agnew, P.; Davis, L.S.; Trice, J.; Jones, C.; et al. Forecasting capabilities for the London 2012 Olympics. *Bull. Am. Meteorol. Soc.* **2014**, *95*, 883–896. [CrossRef]
14. Li, X. Coastal wind analysis based on active radar in Qingdao for Olympic sailing event. In *The International Archives of the Photogrammetry, Remote Sensing and Spatial Information Sciences*; ISPRS: Bejing, China, 2008; Volume 37, pp. 653–658.
15. Giannaros, T.M.; Kotroni, V.; Lagouvardos, K.; Dellis, D.; Tsanakas, P.; Mavrellis, G.; Symeonidis, P.; Vakkas, T. Ultrahigh resolution wind forecasting for the sailing events at the Rio de Janeiro 2016 Summer Olympic Games. *Meteorol. Appl.* **2018**, *25*, 86–93. [CrossRef]
16. Spark, E.; Connor, G.J. Wind forecasting for the sailing events at the Sydney 2000 Olympic and Paralympic Games. *Weather Forecast.* **2004**, *19*, 181–199. [CrossRef]
17. Messager, C.; Badham, R.C.; Honnorat, M.; Vandenberghe, F.; Waterhouse, T.; Currie, I. Weather forecast for the 35th America's Cup (2017) winners based on a limited area model. *Meteorol. Appl.* **2020**, *27*, e1879. [CrossRef]
18. Tagliaferri, F.; Viola, I.M. A real-time strategy-decision program for sailing yacht races. *Ocean Eng.* **2017**, *134*, 129–139. [CrossRef]
19. Pezzoli, A.; Bellasio, R. Analysis of Wind Data for Sports Performance Design: A Case Study for Sailing Sports. *Sports* **2014**, *2*, 99–130. [CrossRef]
20. Kikuchi, Y.; Arakawa, S.; Kimur, F.; Shirasaki, K.; Nagano, Y. Numerical study on the effects of mountains on the land and sea breeze circulation in the Kanto district. *J. Meteorol. Soc. Jpn.* **1981**, *59*, 723–738. [CrossRef]
21. Hinata, H.; Yanagi, T.; Takao, T.; Kawamura, H. Wind-induced Kuroshio warm water intrusion into Sagami Bay. *J. Geophys. Res.* **2005**, *110*. [CrossRef]
22. Weather Research and Forecasting Model. Available online: https://www.mmm.ucar.edu/weather-research-and-forecasting-model (accessed on 22 October 2020).
23. Scire, J.S.; Robe, F.R.; Fernau, M.E.; Yamartino, R.J. *A User's Guide for the CALMET Meteorological Model (Version 5.0)*; Earth Tech Inc.: Concord, MA, USA, 1999.
24. Bellasio, R.; Maffeis, G.; Scire, J.S.; Longoni, M.G.; Bianconi, R.; Quaranta, N. Algorithms to Account for Topographic Shading Effects and Surface Temperature Dependence on Terrain Elevation in Diagnostic Meteorological Models. *Bound. Layer Meteorol.* **2005**, *114*, 595–614. [CrossRef]
25. Schlager, C.; Kirchengast, G.; Fuchsberger, J. Empirical high-resolution wind field and gust model in mountainous and hilly terrain based on the dense WegenerNet station networks. *Atmos. Meas. Tech.* **2018**, *11*, 5607–5627. [CrossRef]
26. Schlager, C.; Kirchengast, G.; Fuchsberger, J. Generation of high-resolution wind fields from the dense meteorological station network WegenerNet in south-eastern Austria. *Weather Forecast.* **2017**, *32*, 1301–1319. [CrossRef]
27. WindRose PRO3. Available online: https://www.enviroware.com/portfolio/windrose-pro3/ (accessed on 22 October 2020).
28. Moriarity, R.J.; Liberda, E.N.; Tsuji, L.J. Using a geographic information system to assess local scale methylmercury exposure from fish in nine communities of the Eeyou Istchee territory (James Bay, Quebec, Canada). *Environ. Res.* **2020**, *191*, 110147. [CrossRef]
29. Lu, B.; Stocks, M.; Blakers, A.; Anderson, K. Geographic information system algorithms to locate prospective sites for pumped hydro energy storage. *Appl. Energy* **2018**, *222*, 300–312. [CrossRef]
30. Dijkink, S.; Winchell, R.J.; Krijnen, P.; Schipper, I.B. Quantification of Trauma Center Access Using Geographical Information System–Based Technology. *Value Health* **2020**, *23*, 1020–1026. [CrossRef]
31. Zambrano, L.I.; Rodriguez, E.; Espinoza-Salvado, I.A.; Fuentes-Barahona, I.C.; de Oliveira, T.L.; da Veiga, G.L.; da Silva, J.C.; Valle-Reconco, J.A.; Rodríguez-Morales, A.J. Spatial distribution of dengue in Honduras during 2016–2019 using a geographic information systems (GIS)–Dengue epidemic implications for public health and travel medicine. *Travel Med. Infect. Dis.* **2019**, *32*, 101517. [CrossRef]

32. Ogato, G.S.; Bantider, A.; Abebe, K.; Geneletti, D. Geographic information system (GIS)-Based multicriteria analysis of flooding hazard and risk in Ambo Town and its watershed, West shoa zone, oromia regional State, Ethiopia. *J. Hydrol. Reg. Stud.* **2020**, *27*, 100659. [CrossRef]
33. Hossain, M.S.; Gadagamma, C.K.; Bhattacharya, Y.; Numada, M.; Morimura, N.; Meguro, K. Integration of smart watch and Geographic Information System (GIS) to identify post-earthquake critical rescue area part. I. Development of the system. *Prog. Disaster Sci.* **2020**, *7*, 100116. [CrossRef]
34. Amazon Web Services. Available online: https://aws.amazon.com/it/what-is-aws/ (accessed on 22 October 2020).
35. SRTM Data. Available online: https://www2.jpl.nasa.gov/srtm/ (accessed on 22 October 2020).
36. JAXA Land Use Data. Available online: https://www.eorc.jaxa.jp/ALOS/en/lulc/lulc_index.htm (accessed on 22 October 2020).
37. Dudhia, J. Numerical study of convection observed during the Winter Monsoon Experiment using a mesoscale two-dimensional model. *J. Atmos. Sci.* **1989**, *46*, 3077–3107. [CrossRef]
38. Kain, J.S.; Kain, J. The Kain—Fritsch convective parameterization: An update. *J. Appl. Meteorol.* **2004**, *43*, 170–181. [CrossRef]
39. Hong, S.-Y.; Noh, Y.; Dudhia, J. A new vertical diffusion package with an explicit treatment of entrainment processes. *Mon. Weather. Rev.* **2006**, *134*, 2318–2341. [CrossRef]
40. Mlawer, E.J.; Taubman, S.J.; Brown, P.D.; Iacono, M.J.; Clough, S.A. Radiative transfer for inhomogeneous atmospheres: RRTM, a validated correlated-k model for the longwave. *J. Geophys. Res. Atmos.* **1997**, *102*, 16663–16682. [CrossRef]
41. Lin, Y.; Farley, R.; Orville, H. Bulk Parameterization of the Snow Field in a Cloud Model. *J. Clim. Appl. Meteorol.* **1983**, *22*, 1065–1092. [CrossRef]
42. Powell, M.D.; Rinard, S.K. Marine forecasting at the 1996 centennial Olympic games. *Weather Forecast.* **1998**, *13*, 764–782. [CrossRef]
43. Ma, Y.; Gao, R.; Xue, Y.; Yang, Y.; Wang, X.; Liu, B.; Xu, X.; Liu, X.; Hou, J.; Lin, H. Weather support for the 2008 Olympic and Paralympic sailing events. *Adv. Meteorol.* **2013**, *2013*, 289284. [CrossRef]
44. Bai, Y.; Li, Y.; Wang, X.; Xie, J.; Li, C. Air pollutants concentrations forecasting using back propagation neural network based on wavelet decomposition with meteorological conditions. *Atmos. Pollut. Res.* **2016**, *7*, 557–566. [CrossRef]
45. Hernández, A.; Saavedra, S.; Rodríguez, A.; Souto, J.A.; Casares, J.J. Coupling WRF and CALMET models: Validation during primary pollutants glc episodes in an Atlantic coastal region. In *Air Pollution Modeling and Its Application*, 22nd ed.; Springer: Dordrecht, The Netherlands, 2014; pp. 681–684.
46. Sun, W.; Sun, J. Daily PM2. 5 concentration prediction based on principal component analysis and LSSVM optimized by cuckoo search algorithm. *J. Environ. Manag.* **2017**, *188*, 144–152. [CrossRef] [PubMed]
47. González, J.A.; Hernández-Garcés, A.; Rodríguez, A.; Saavedra, S.; Casares, J.J. Surface and upper-air WRF-CALMET simulations assessment over a coastal and complex terrain area. *Int. J. Environ. Pollut.* **2015**, *5*, 249–260. [CrossRef]
48. Houghton, D.; Campbell, F. *Wind Strategy*, 3rd ed.; John Wiley & Sons Inc.: London, UK, 2006.